Journal of Wind Engineering & Industrial Aerodynamics 222 (2022) 104889

Contents lists available at ScienceDirect

Journal of Wind Engineering & Industrial Aerodynamics

journal homepage: www.elsevier.com/locate/jweia

Optimization of long-span suspension bridge erection procedure considering flutter risk in mixed extreme wind events

Ma Teng [a,b], Cui Wei [a,b,c,*], Zhao Lin [a,b,c,d], Yang Yongxin [a,b,c], Ge Yaojun [a,b,c]

[a] State Key Lab of Disaster Reduction in Civil Engineering, Tongji University, Shanghai 200092, China
[b] Department of Bridge Engineering, College of Civil Engineering, Tongji University, Shanghai 200092, China
[c] Key Laboratory of Transport Industry of Bridge Wind Resistance Technologies, Tongji University, Shanghai 200092, China
[d] State Key Laboratory of Mountain Bridge and Tunnel Engineering, Chongqing Jiaotong University, Chongqing, 400074, China

ARTICLE INFO

Keywords:
Long span bridge
Flutter risk probability
Deck erection
Mixed wind climate

ABSTRACT

During the erection stage of the suspension bridge, its critical flutter wind speed is continuously varying due to changing structural dynamic properties including mass and stiffness. On the other hand, the wind climate is also varying greatly seasonally or even monthly during the bridge erection procedure. This work proposes an analytical framework to optimize the deck erection timeline under complex wind climate attacks. Xihoumen Bridge built at Chinese southeastern coast is taken as a calculation example. Full-bridge aeroelastic model wind tunnel test was conducted to examine the critical flutter speed at different erection stages. Extreme wind speed for tropical cyclones and synoptic wind are analyzed by tropical cyclone simulation and meteorological records respectively. Results show that the optimal timeline for Xihoumen Bridge is starting in August if a one-month duration is required for each stage. However, if the worst timeline is selected, the flutter risk will be increased 40 times larger. If the construction timeline is flexible for the construction schedule, this research proves that timeline optimization is a more economical and safe approach than structural approaches like storm ropes.

1. Introduction

The bridges with the longest span around the world are all suspension bridges due to their advanced structural capability both in design and construction. However, for this superior structure, aerodynamic stability is a safety control factor since the collapse of the Tacoma Narrow Bridge (Amman et al., 1941). To verify and study the wind-induced stability of suspension bridges, wind tunnel tests, numerical simulation, and theoretical analysis are generally used. These methods can evaluate the critical flutter wind speed of bridge sections under certain dynamic characteristics, thus ensuring safety during the bridge life-cycle.

In addition, the danger of wind-induced instability also occurs during the erection stage of the deck, which is more vulnerable because of incomplete structures. The overall stiffness of a suspension bridge at its erection stage is significantly smaller than that when it is completely constructed, primarily due to the lack of overall torsional stiffness continuity of the deck. Therefore, the general conditions against the aerodynamic instability are found to be less favorable than the final stage (Tanaka et al., 1998). Since the 1960s, a lot of bridges are tested in boundary layer wind tunnels to ensure their safety during the deck erection phase, such as the Severn Bridge in England (Smith, 1964), the Great Belt Bridge in Denmark (Larsen, 1993) and the Xihoumen Bridge in China (Yang et al., 2018). Some significant factors governing the aeroelastic stability are discussed by previous research including dynamic properties (Tanaka et al., 1998; Ge and Tanaka, 2000), vibration mode shapes (Svensson and Kovacs, 2017), mass eccentricity (Larsen, 1997) and erection sequences (Arco and Aparicio, 2001). Bridge flutter risk in the construction stage is a time-varying process due to its continuously changing structural status.

Generally, wind-induced instability of suspension bridges under erection could be precluded by avoiding extreme weather period, such as tropical cyclone (Chen et al., 1997). However, with the increasing of the bridge span the deck erection period becomes longer and longer, even more than one year like Akashi Kaikyo Bridge (Miyata and Yamaguchi, 1993). For modern ultra long-span suspension bridges, it is inevitable to continue constructing bridges over tropical cyclones season.

To strengthen aerodynamic stability during construction, some structural and aerodynamic measures are proposed such as storm ropes (Yang et al., 2018) and aerodynamic stabilizer (Bakis et al., 2016).

* Correspondence to: Tongji University, 320 Wind Engineering Building, 1239 Siping Road, Shanghai, 200092, China.
E-mail addresses: tengma@tongji.edu.cn (Ma T.), cuiwei@tongji.edu.cn (Cui W.), zhaolin@tongji.edu.cn (Zhao L.), yangyongxin@tongji.edu.cn (Yang Y.), yaojunge@tongji.edu.cn (Ge Y.).

https://doi.org/10.1016/j.jweia.2021.104889
Received 25 August 2021; Received in revised form 28 November 2021; Accepted 28 December 2021
Available online 1 February 2022

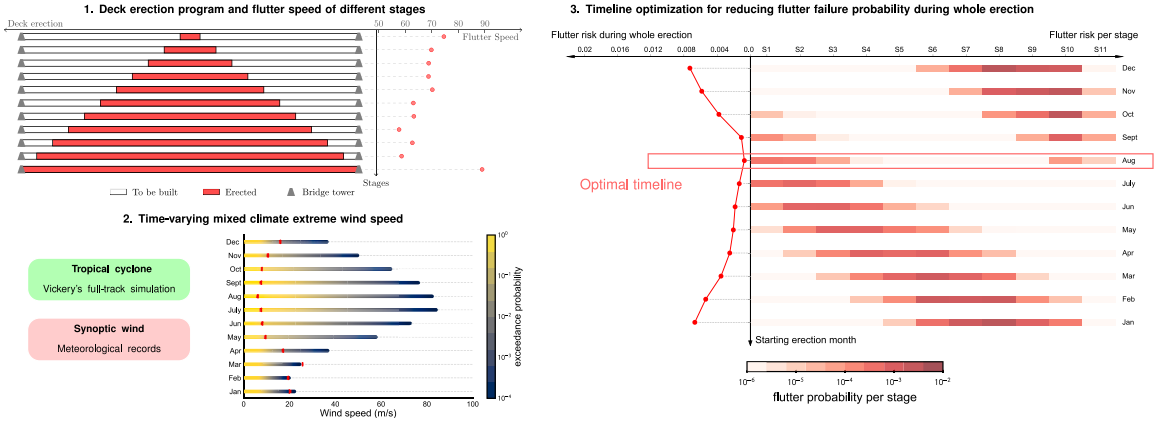

Fig. 1. Schematic of long-span suspension bridge deck erection timeline optimization considering mixed wind climate attacking.

Choosing appropriate deck erection sequences is another method to reduce flutter risk during construction. Previous research (Yang et al., 2018) focuses on improving the most adverse flutter critical wind speed during construction. However, continuous time-varying in aerodynamic stability performance and wind climate will happen simultaneously during the deck erection procedure. Deck erection procedure should be optimized in such a mixed and time-varying wind climate to minimize the bridge aerodynamic flutter on-site risk during the whole deck erection process.

Extreme wind speed exceeding probability is varying strongly in different seasons especially in mixed wind climate regions composed of tropical cyclones and synoptic winds. Mixed climate regions are affected by a variety of wind climates effects, like tropical cyclone zone affected by a tropical cyclone and monsoon (Habte et al., 2015) and mountainous zone affected by diurnal and synoptic winds. This study focuses on tropical cyclones and monsoon mixed zone, like China's southeast coastal and Japan. The seasonality of tropical cyclones causes the wind speed exceeding probability function to be time-dependent at different stages of construction.

The technique for mixed wind climate extreme wind speed calculation required a separate extreme-value analysis (Cui et al., 2021; Chen and Lombardo, 2020) of the values stemming from each significant wind-producing mechanism, followed by synthesis of the individual mechanisms into a composite extreme-value distribution. Gomes and Vickery (1978) carried out the different causative mechanisms of extreme wind speed analysis for Australia and America. Synoptic wind speeds are recorded by meteorological observatory (Young et al., 2018), but for tropical cyclones, the size of the available data sample is normally too small to perform extreme-value analysis. So several data-driven simulation methods have been developed for tropical cyclone simulation in wind engineering (Vickery et al., 2000b,a; Scanlan and Simiu, 1996; Georgiou, 1986). Recently, Vickery's empirical track model has been widely adopted (Cui and Caracoglia, 2019; Fang et al., 2021; Chu et al., 2021) to incorporate season change effects on tropical cyclone simulation.

The present paper proposes a bridge deck erection procedure optimization method considering flutter risk in a time-varying mixed wind climate. Xihoumen bridge is employed by this study as an engineering application example. Bridge aerodynamic flutter stability for each construction stage has been tested by a full-model wind tunnel test. Next, time-varying mixed wind climate is evaluated as extreme wind speed annual exceed probability distribution function (PDF) for each month. Synoptic wind speed analysis data sample is extracted from NOAA Global Integrated Surface Dataset. On the other hand, tropical cyclone wind speeds are simulated by Vickery's full track Monte Carlo simulation. Probability theory for independent events from two wind climate mechanisms is used to calculate the mixed extreme wind speed governed by tropical cyclones and monsoon. Then, an optimization algorithm is used to search for the best deck erection starting timeline for different bridge erection procedures to minimize the bridge flutter on-site probability during the whole deck erection construction process. Two specific analysis methods and visualizations are proposed in Section 4. Flutter risk flow is used to describe single program flutter performance and erection flutter risk box-plot is a horizontal comparison tool of different erection processes. At last, several topics are discussed, including how to choose the better deck erection plan for different erection procedure configurations.

The paper is outlined as follows. Firstly, full model wind-tunnel tests of the Xihoumen bridge at its deck erection stage are described in Section 2 to investigate flutter stability experimentally. Section 3 provides the extreme wind speed exceeding probability calculation by meteorological wind speed data and Vickery's full track Monte Carlo tropical cyclone simulation. Then, the time-varying flutter limit and the time-varying extreme wind speed are incorporated in Section 4 to obtain the lowest flutter risk in the whole construction process. Section 5 discusses several further topics for erection timeline optimization and erection plan selecting a strategy. At last, Some basic conclusion is presented in Section 6. The schematic of this paper is shown in Fig. 1.

2. Flutter risk during deck erection by wind tunnel test

Xihoumen bridge is a three-span slotted-box girder suspension bridge with a main span of 1650 m. In this paper, the Xihoumen bridge is employed as a classical suspension case to study aerodynamic flutter limits in different deck erection stages. Xihoumen Bridge was constructed in December 2007, and the wind engineering consulting was performed by the State Key Lab of Disaster Reduction in Civil Engineering in Tongji University. The wind tunnel test results for different erection stages are retrieved as the benchmark project in this study.

2.1. Wind-tunnel test setup

The elevation of the Xihoumen bridge and main girder section are shown in Figs. 2 and 3. Limit to wind tunnel size, its full aerodynamic model was designed and manufactured with the geometrical scale of 1:208. The structural parameters of the model including geometrical dimensions, mass characteristics, and fundamental frequencies were listed in Table 1. The wind-tunnel test was conducted in the TJ-3 boundary layer wind tunnel of the State Key Laboratory of Disaster Reduction in Civil Engineering at Tongji University, which is 15 m wide, 2 m high, 14 m long and could replicate the wind velocity up to 17.6 m/s. The wind tunnel test is shown in Fig. 4.

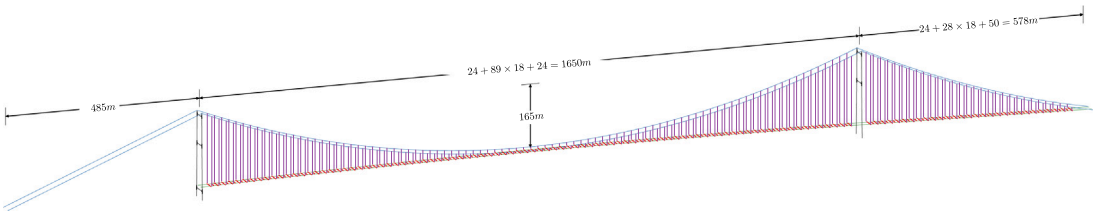

Fig. 2. Elevation of the Xihoumen bridge.

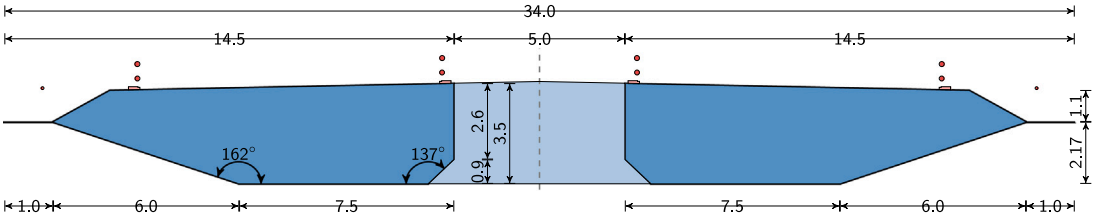

Fig. 3. Central-slotted box girder of Xihoumen bridge.

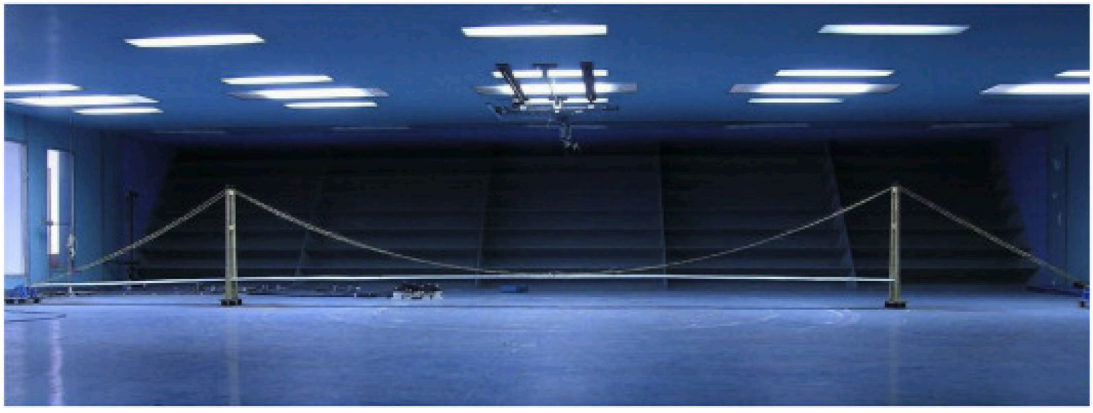

Fig. 4. The full model of Xihoumen bridge in TJ-3 wind tunnel.

Table 1
Structural parameters of objective model.

Parameter	Unit	Prototype		Scaling	Model
Length(L)	m	Deck	578+1650+485	$\lambda_L = 1:208$	2.779+7.9033+2.332
Width(B)	m	Deck	36.000	$\lambda_L = 1:208$	0.173
Depth(H)	m	Deck	3.538	$\lambda_L = 1:208$	0.017
Mass(m)	kg/m	Deck	1.691×10^4~1.731×10^4	$\lambda_m = 1:208^2$	0.391 ~ 0.400
		Main cables	3.879×10^3~4.017×10^3		8.967×10^{-2} ~ 9.285×10^{-2}
Mass moment(J_m)	kg m^2/m	Deck	1.936×10^6~2.036×10^6	$\lambda_m = 1:208^4$	1.034×10^{-3} ~ 1.088×10^{-3}
Cross-section area(A)	m^2	Main cables	0.46460~0.48110	$\lambda_m = 1:208^2$	1.074×10^{-5} ~ 1.112×10^{-5}
		Hangers	0.00726		1.678×10^{-7}
Tensile stiffness(EA)	N	Main cables	9.262×10^{10}~9.622×10^{10}	$\lambda_m = 1:208^3$	1.033×10^4 ~ 1.069×10^4
		Hangers	1.016×10^9		1.129×10^2
Vertical bending stiffness(EI_z)	N m^2	Deck	2.101×10^{12}	$\lambda_{EI} = 1:208^5$	5.397
Lateral bending stiffness(EI_y)	N m^2	Deck	1.190×10^{14}	$\lambda_{EI} = 1:208^5$	3.057×10^2
Torsional stiffness(GJ_d)	N m^2	Deck	4.628×10^{12}	$\lambda_{EI} = 1:208^5$	11.887
Vertical bending frequency(f_h)	Hz		0.1005	$\lambda_f = \sqrt{208}:1$	1.4491
Lateral bending frequency(f_p)	Hz		0.0485	$\lambda_f = \sqrt{208}:1$	0.7001
Torsional frequency(f_h)	Hz		0.2321	$\lambda_f = \sqrt{208}:1$	3.3478

2.2. Case list and result

Normally, there are three different Deck erection of suspension bridges: mid-span to pylons, pylons to mid-span, and combining both above methods. Generally, box-girder suspension bridges are constructed from mid-span to pylons, such as the Humen Bridge and the Jiangyin Bridge. In addition to practical experience, some research proved its advantages theoretically, including construction process (Gimsing and Georgakis, 2011) and mechanical behavior (Tanaka and Gimsing, 1999). So mid-span to pylons is also used in this study as the long-span suspension bridge deck erection process.

Accordingly, the sequence of mid-span to pylons is applied here with two different deck erection programs: symmetric and asymmetric. The according erection programs are displayed in the left part of Figs. 5 and 6. Flutter speeds for different deck erection stages is shown in the right part of Figs. 5, 6. The critical flutter speed of the bridge under construction is clearly lower than that of the final stage, which

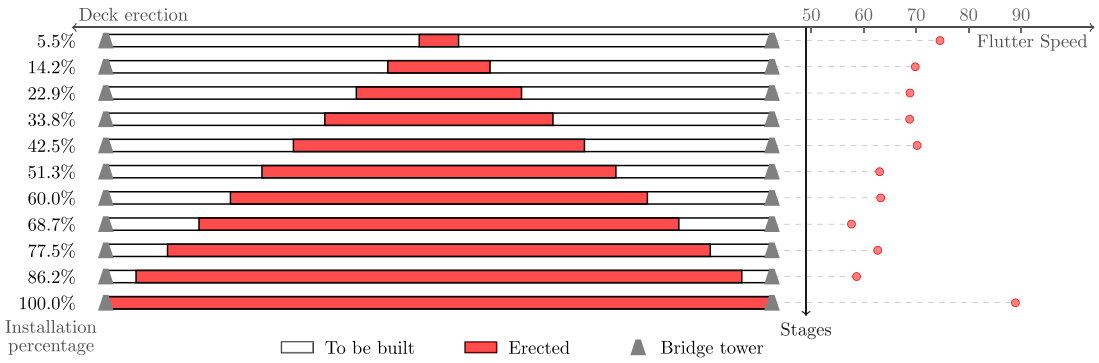

Fig. 5. Symmetric deck erection program and flutter velocities of different stages.

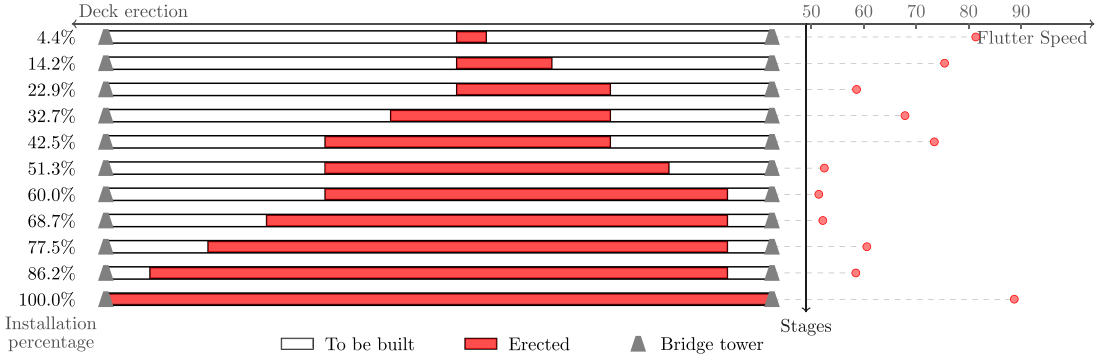

Fig. 6. Asymmetric deck erection program and flutter velocities of different stages.

confirmed that the aerodynamic stability of suspension bridges does degenerate during deck erection. Furthermore, the critical flutter speed is time-varying from 50 m/s to 80 m/s during construction. The change of flutter wind speed during bridge construction is related to dynamic characteristics and bridge section shape.

3. Mixture climate extreme wind speed in different months

Extreme wind speed calculation in mixed wind climate requires a separate extreme-value analysis of the values stemming from each significant wind-producing mechanism, followed by synthesis of the individual mechanisms into a composite extreme-value distribution. Since lots of long-span suspension bridges are built in coastal areas, this paper focuses on the wind climate composed of tropical cyclones and synoptic wind. Time-varying wind climate is considered as extreme wind speed annual exceed probability distribution function for each month. NOAA Global Integrated Surface Dataset is used to fit synoptic wind distribution while tropical cyclone simulation is for tropical cyclone dataset.

3.1. Vickery's full-track simulation model

Tropical cyclone simulation is required to appropriately evaluate the wind speed at a specific place. Because the actual tropical cyclone samples are too few to perform reliable extreme value analysis. Vickery's model (Vickery et al., 2000b,a) is a powerful tool, in this case, utilizing statistical properties of tropical cyclones' initiations, tracks, and intensities from history to generate simulated tropical cyclone results, from which the extreme tropical cyclone wind speeds can be calculated.

Vickery's track model simulates the tropical cyclone translation velocity c, heading θ and the relative intensity I. These quantities are expressed in Eqs. (1), (2) and (3):

$$\Delta lnc = a_1 + a_2\Phi + a_3\lambda + a_4 lnc_i + a_5\theta_i + \epsilon_c \tag{1}$$

$$\Delta\theta = b_1 + b_2\Phi + b_3\lambda + b_4 lnb_i + b_5\theta_i + \epsilon_\theta \tag{2}$$

$$ln(I_{i+1}) = c_0 + c_1 ln(I_i) + c_2 ln(I_{i-1}) + c_3 ln(I_{i-2}) + c_4 T_s + c_5(\Delta T_s) + \epsilon_I \tag{3}$$

where $a_i (i = 1, 2, \ldots, 5)$ and $b_i (i = 1, 2, \ldots, 6)$ are coefficients obtained by regression analysis from historical records; Φ and λ are latitude and longitude of the tropical cyclone center, respectively; c_i is the tropical cyclone translation speed at time step i; θ_i is the tropical cyclone heading at time step i, range of which is $-180°$ to $180°$, and $\theta = 0$ when the tropical cyclone is heading north; ΔT_s is sea surface temperature difference between time step i and $i + 1$; I is the relative intensity I, utilized to relate the actual tropical cyclone pressure deficit Δp to the greatest possible central pressure deficit allowed by the average climatology of the tropical cyclone season (Vickery et al., 2000b); ϵ_c, ϵ_θ and ϵ_I are linear regression residuals.

The intensity decay model is utilized to describe energy decreasing after tropical cyclone landing. It is expressed as

$$\Delta p(t) = \Delta p_0 e^{-at_h} \tag{4}$$

$$a = a_0 + a_1 \Delta p + \epsilon_a \tag{5}$$

where $\Delta p(t)$ is the central pressure deficit; Δp_0 is the pressure deficit when the tropical cyclone lands; a is the exponential decay rate over time t_h; a_0, a_1 are site-specific parameters; ϵ_a is residual.

20 000 years tropical cyclone simulation is created by Vickery's full-track simulation model. The tropical cyclone data at a specific bridge site is obtained from the track information. The maximum wind speed of each track within 300 km of the bridge site is captured to fit the extreme-value distribution.

Method of independent storms (MIS) proposed by Cook (1982) and Harris (1999) is used to do extreme-value analysis for tropical cyclone. The extreme wind speed sample is composed of the maximum wind speed in each storm. Data sample is fitted by Gumbel

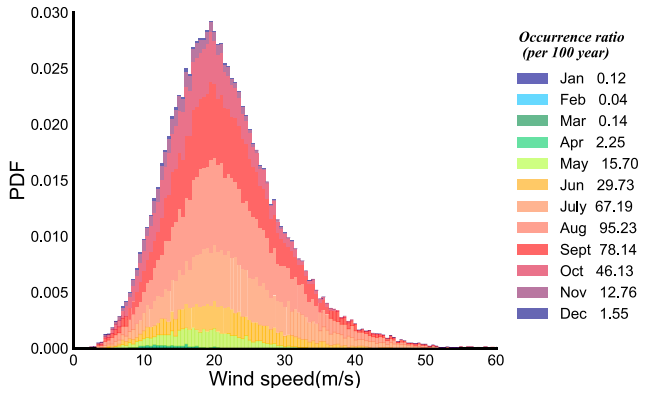

Fig. 7. Tropical cyclone wind speed distribution of different months at Xihoumen bridge site.

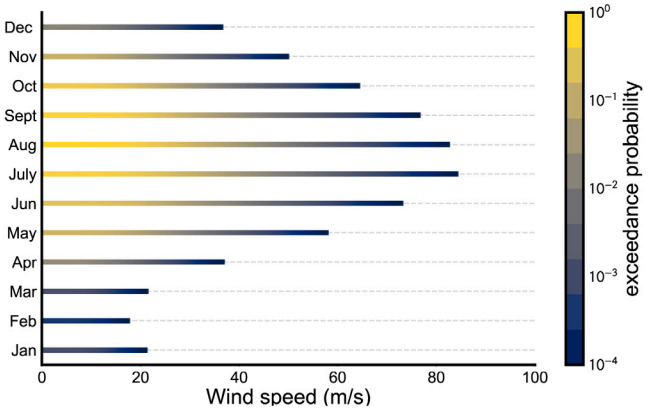

Fig. 8. Tropical cyclone wind speed exceeding probability in different months at Xihoumen bridge site.

distribution (Gumbel, 2004), whose cumulative distribution function is expressed below:

$$P(u \le U) = \exp\left[-\exp\left(-\frac{U-\beta}{\alpha}\right)\right] \tag{6}$$

where β is the location parameter and α is the scale parameter. The extreme wind speed exceed probability in epoch T could be calculated by the Poisson process:

$$P_T(u \le U) = \sum_{i=0}^{\infty} \frac{P(u \le U)^i [rT]^i \exp(-rT)}{i!} = \exp\{-rT[(1 - P(u \le U))]\} \tag{7}$$

where i is the number of occurrences, r is the rate of independent events per unit time, T is the epoch, and $P(u \le U)$ is the Cumulative Distribution Function of Gumbel distribution fitted by tropical cyclone extreme wind speed sample.

Zhoushan, where the Xihoumen bridge site is located, is used as a calculation case. The distribution of tropical cyclone wind speed occurring 12 months is shown as Fig. 7. August, September, and July have higher tropical cyclone frequency and intensity. The extreme wind speed exceeding probability in different months could be calculated by Eq. (7) and the result is shown as Fig. 8. It can be clearly seen that the extreme wind speed is dependent on season or month strongly. Tropical cyclone wind speed with an exceeding probability of 0.0001 is 18 m/s in February, but 83 m/s in July.

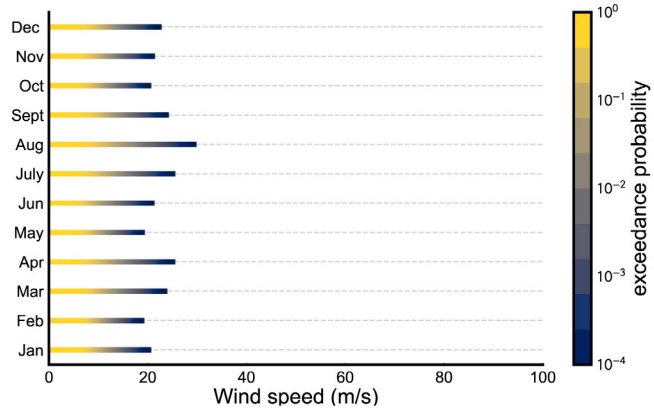

Fig. 9. Synoptic wind speed exceeding probability in different months at Xihoumen bridge site.

3.2. Synoptic extreme wind speed

In addition to tropical cyclones, synoptic extreme wind speed is also important for extreme wind climate. Synoptic wind speed is extracted from NOAA Global Integrated Surface Dataset (Young et al., 2018). This database covers wind observation, hourly liquid precipitation, sky condition, air temperature, sea level pressure, and etc. Synoptic wind speed exceeding probability is calculated by stage maximum method per year. The stage maximum method is the most widely used in wind-resistance code around the world (ASCE, 2016; Ministry of Transports of the People's Republic of China, 2018).

In this case, the extreme-value sample is composed by maximum wind speed excluding tropical cyclone records and then divided into 12 groups by month. Each group is used to fit Gumbel distribution separately (Eq. (6)). The exceeding probability of synoptic wind speed is the Cumulative Distribution Function of Gumbel distribution.

For Zhoushan city, a synoptic wind speed sample is recorded at DINGHAI station (NO.584770) of NOAA Global Integrated Surface Dataset. The extreme wind speed exceeding probabilities in different months result are shown in Fig. 9. Compared to a tropical cyclone, the synoptic wind is less intense, and the seasonal variation is not obvious.

3.3. Mixed extreme wind speed

Coastal long-span suspension bridge site is affected by mixed wind climate composed of tropical cyclone(T) and synoptic wind(N). The cumulative probability $P_t(u \le U)$ of the maximum value u from either mechanism in an epoch t is less than any specific value U could be calculated by:

$$P_t(u \le U) = P_t(u_N \le U) \times P_t(u_T \le U) \tag{8}$$

where u_N, u_T is the wind speed from mechanism synoptic wind and tropical cyclone.

Fig. 10 shows the extreme value result of mixed wind climate in the Xihoumen bridge site. Compared with the single mechanism extreme-value analysis result, it is the envelope of two single mechanisms curve. The red solid line is the interaction point of tropical cyclone control or synoptic wind control. Synoptic wind normally controls low exceeding probability(or called low return period). More tropical cyclone occurs, the cut-off point moves more left. The cut-off point schematic of tropical cyclone control and synoptic wind control is shown in Fig. 11. So coastal mixed wind climate is strongly seasonal related due to tropical cyclones.

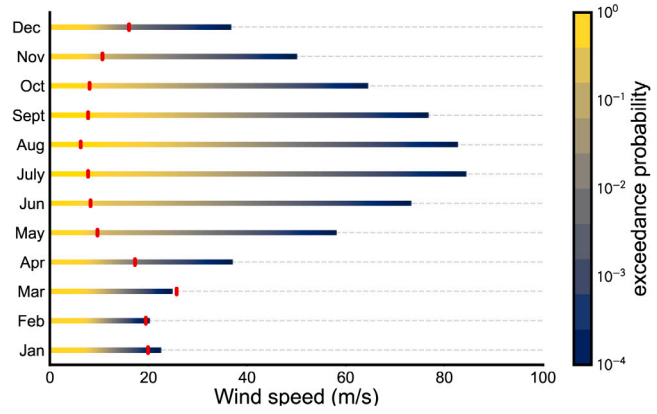

Fig. 10. Mixed wind speed exceeding probability in different months at Xihoumen bridge site (red solid line is the cut-off point of tropical cyclone control and synoptic wind control).

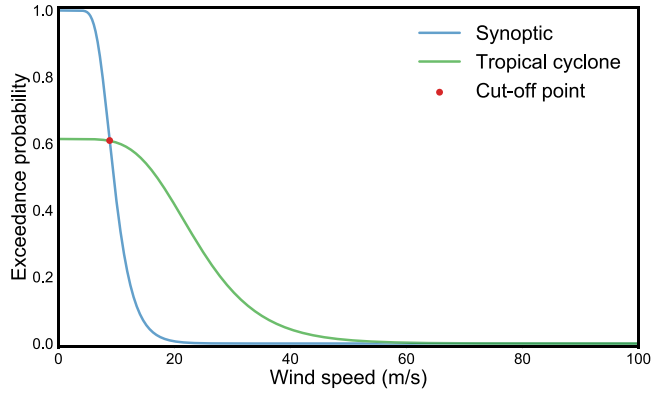

Fig. 11. Cut-off point schematic of tropical cyclone control and synoptic wind control.

4. Flutter failure probability during whole erection

Long-span suspension bridge flutter failure risk during erection is a strongly state-dependent process. Critical flutter speed is continuous time-varying during erection and wind climate is also changing in different months because of tropical cyclones. In previous research, aerodynamic instability during erection is considered conservatively whose the lowest flutter speed state is used as a critical metric. On the other hand, annual extreme wind speeds PDF is used rather than PDF per month. In this section, the flutter failure is calculated as the total probability during erection considering all possible erection states. Some factors related to flutter probability are discussed and optimized, including starting erection month, erection program, and erection speed.

4.1. Flutter probability calculation

Flutter failure in a single stage is defined as the probability of extreme wind speed exceeding flutter speed testing by wind tunnel test. Extreme-value wind speed distribution is independent. So the flutter probability of single-stage P_i could be calculated as:

$$P_i = 1 - \prod_{i=m}^{m+t} P(u_i \le U) \tag{9}$$

where i is the current month and $P(u_i \le U)$ is the cumulative distribution function of extreme wind speed distribution in i month calculated by Eq. (7); m is the start month of this stage; t means the erection stage duration. If one stage lasts less than one month, T in Eq. (7) will be the percentage of time that this stage stays in the month.

Flutter critical wind speed is independent in different construction stages. So flutter probability during whole erection is opposing events of no flutter occur in each construction stage, which could express as:

$$P(\text{flutter}) = 1 - \prod_{i=0}^{n} P_i \tag{10}$$

where P_i is the probability of flutter occur in stage i calculated by Eq. (9).

4.2. Optimization of starting erection month

Optimizing bridge deck erection process is performed to select ideal erection starting month to reduce the probability of flutter failure during construction. In addition, this research assumes that the bridge erection process is continuous, with no gaps between the two stages. When to start erection can be optimized to avoid that adverse wind conditions and adverse the erection state with high flutter risk would happen at the same time.

For a certain construction plan, including the girder erection process and the girder erection cycle, there must be an optimal start time. Flutter risk flow is defined to choose the optimal start month and the lowest flutter failure probability. The flutter risk flow contains the stage flutter risks and total flutter risk for different starting months.

Taking Xihoumen bridge as an example, the flutter risk flow of symmetry and asymmetric construction process are calculated and shown in Figs. 12 and 13, respectively. Critical flutter speeds are from the full bridge model wind tunnel test described in Section 2. Extreme-value wind speed is calculated by mixed wind climate theory in Section 3. Flutter risk is calculated by assuming each stage costs one month.

Flutter risk flow example is shown as Figs. 12, 13. For each candidate deck erection program, flutter failure probability during one stage and the whole process is given in one row of flutter risk flow. Flutter probability during one stage is in the right part of flutter risk flow, which is represented by a heat map. Whole deck erection flutter failure is in the left part of flutter risk flow, which is represented by scatter plots. Flutter risk flow could compare different deck erection programs. Same deck erection program with different start month are compared in Figs. 12, 13, so the vertical axis is the starting erection month.

As shown in Fig. 13, the lowest flutter failure probability is 0.05%, and the highest is 2%. 40 times difference occurs comparing different starting months.

The optimal starting month is August for Xihoumen deck erection symmetric and asymmetric process from flutter risk flow analysis. Interestingly, judging from the flutter critical wind speed curve of the construction state alone, the asymmetrical construction plan is worse than the positive symmetric one. The lowest flutter speed of asymmetric is 5 m/s less than symmetric plan.

As illustrated in Fig. 6, stages 6–8 of asymmetric are three consecutive flutter adverse states with 50 m/s flutter speed. But when bridge deck erection starts in August, the optimal start month, symmetric process total flutter failure is 0.072% and asymmetric is 0.05%. From the view of minimum overall failure probability, the asymmetrical construction method is better than the symmetric construction method, when the construction period is 1 month.

4.3. Analysis of erection speed

The optimal start time is affected by the construction speed and construction plan. The exposure time of bridge erection stages in different wind environments is different under various deck erection speeds. The influence of erection speed on the total flutter failure probability will be analyzed in this section.

The flutter flow chart is a good method to evaluate the flutter risk of a specific construction plan. But it is not effective to compare

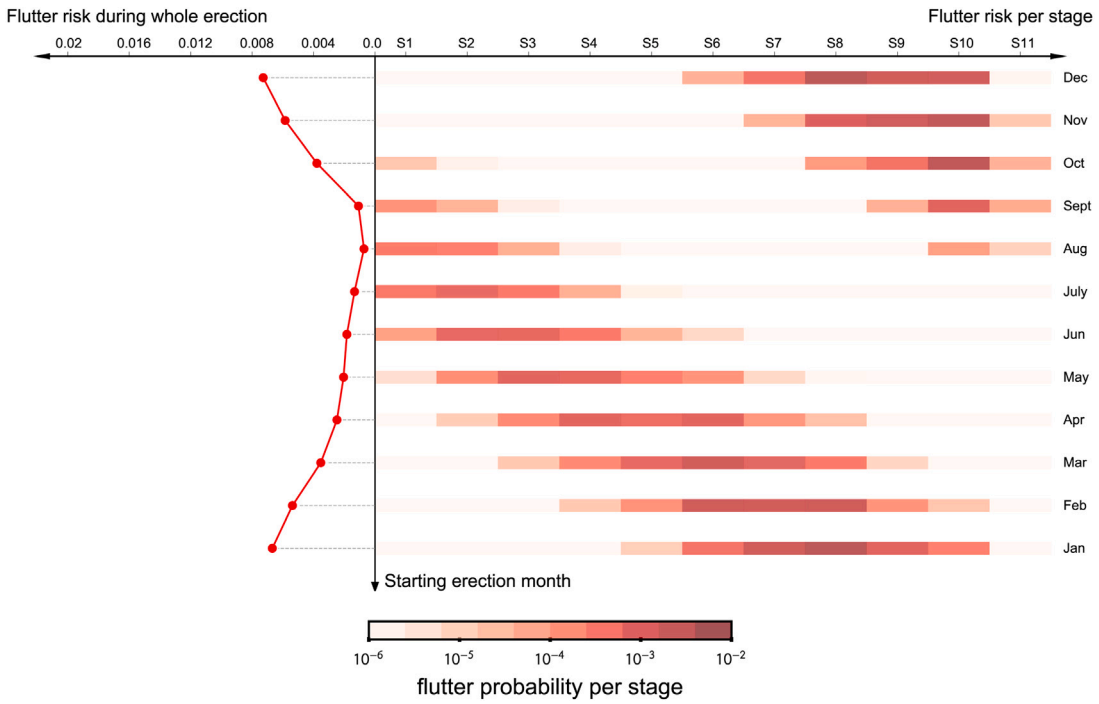

Fig. 12. Flutter risk flow and failure probability with different starting months (symmetric deck erection program).

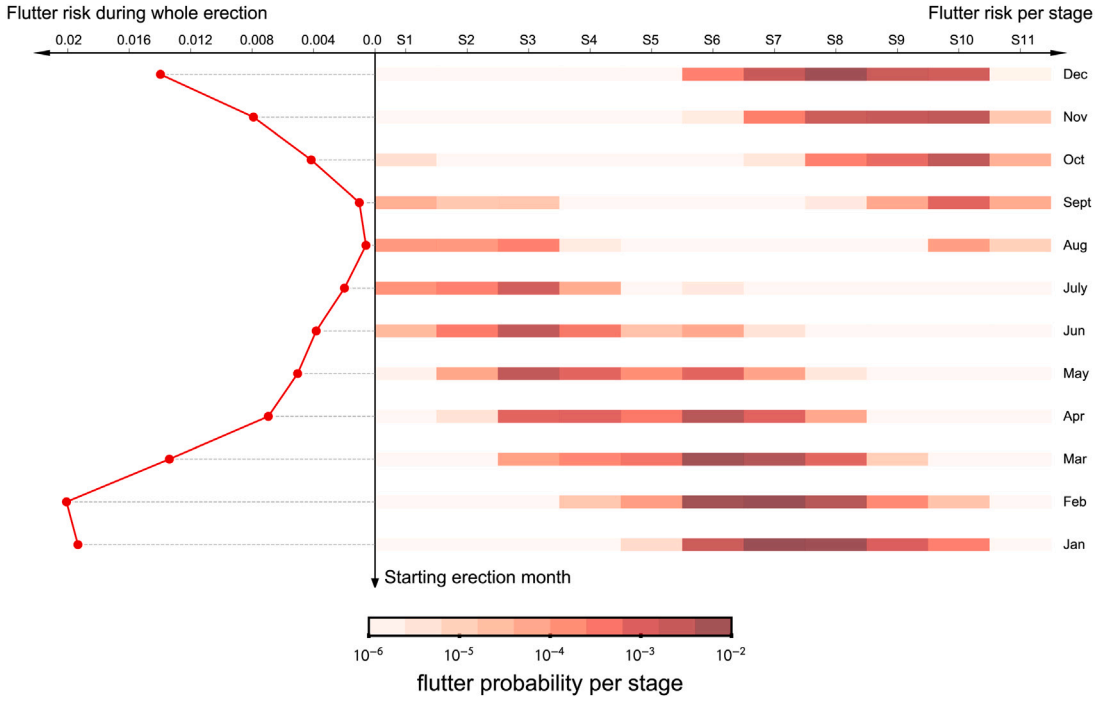

Fig. 13. Flutter risk flow and failure probability with different starting months (asymmetric deck erection program).

among plans with different erection speeds. When a construction plan is determined, the different start times determine its overall flutter risk. A box-plot is drawn in Figs. 14 and 15 to describe all the possible flutter risks with different erection speeds. Different from the general box-plot, the erection flutter box-plot does not have the outlier, because the data is not the sampling of random variables. There are four elements in the erection flutter box-plot, including minimum/maximum flutter failure probability, mean-value of flutter risk, and quartile box. These statistical characteristics are derived from the total flutter risk with different starting months.

Erection flutter risk box-plots of Xihoumen bridge symmetric/asymmetric program are shown in Figs. 14 and 15. The variable for comparison in the box-plot is the speed of erection, that is, the time required for a stage. The y-axis of the figure is the normalized flutter failure probability. With the increase of erection period, the influence of start month on flutter failure probability becomes smaller. Because the impact of the start month is due to seasonal variations of the wind environment will be averaged during each state. When a single state of the structure lasts for a year, the periodic differences disappear. As the construction period increases, the flutter probability of the optimal

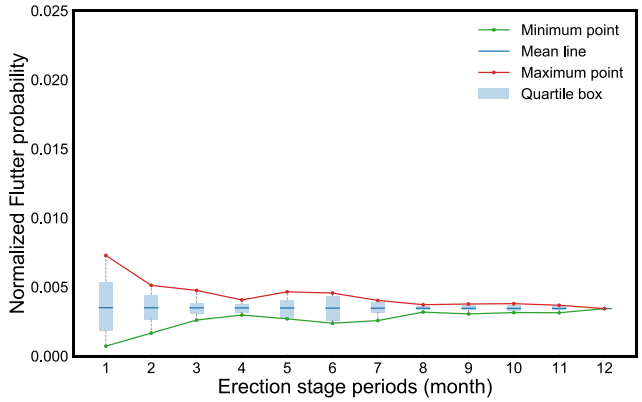

Fig. 14. Normalized flutter risk during erection with different erection stage periods (symmetric deck erection program).

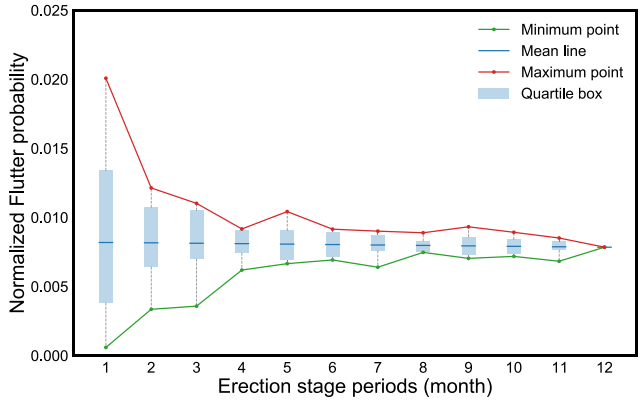

Fig. 15. Normalized flutter risk during erection with different erection stage periods (asymmetric deck erection program).

start date increases gradually, and the flutter probability of the most unfavorable decreases.

5. Discussion

5.1. Erection process decision strategy

In the previous section, flutter risk flow and normalized flutter probability box-plot is proposed to describe and compare total flutter risk of erection processes. In this section, a structural approach is included to improve the counter flutter risk and compared with the methods proposed in this study.

In the traditional wind-resistant design of the bridge construction stage, it is necessary to ensure that the flutter critical wind speed at each stage exceeds the extreme wind speed. The extreme wind speed is normally a 50-years return period extreme wind speed from code or historical record. To pass the requirements of the code, engineers focus only on the most adverse flutter conditions when selecting and optimizing the deck erection process. Some of the irrationality of this approach has been illustrated in the above argument. For example, the asymmetric program has a lower flutter speed but the overall flutter probability is lower than the symmetric program with an optimal erection plan.

The optimal deck erection strategy should have the lowest flutter failure probability in the whole process. The probability of flutter failure during erection is sensitive to the construction timeline because of mixed wind climate, especially the influence of tropical cyclones. In practical engineering, several construction processes and speeds are determined generally. The normalized flutter risk box-plot could be displayed to choose the best program and starting month. And the flutter risk flow could visual the best option to find which stage is dangerous for flutter.

If the unit deck erection period is one month, the best girder erection scheme for Xihoumen Bridge is the anti-symmetric construction program which starts in August. When the start date is limited or the start date cannot be determined in advance, the mean value of the total flutter probability in flutter risk flow should be a good indicator to evaluate the flutter performance of the construction process.

Table 2
Analyzed cases of Xihoumen bridge erection storm ropes.

Label	Storm ropes	Cross-section area
Condition 1	Cable 1	1% A_c
Condition 2	Cable 1	10% A_c
Condition 3	Cable 2	1% A_c
Condition 4	Cable 2	10% A_c

5.2. Structural approach or better timeline

Structural approaches are widely employed to enhance the aerodynamic performance during suspension bridge erection. These methods increase the critical flutter wind speed but increase construction difficulty and cost money. The above illustrates that a decrease in the critical flutter wind speed does not always reduce the total flutter risk during construction. This section discusses whether construction timeline optimization could replace the structural approach to reduce the flutter probability during deck erection.

Eccentric mass is one of the structural approaches to increase flutter speed. Generally, about 20% increase of flutter speed is available by adding an eccentric mass (Brancaleoni and Brotton, 1981; Larsen, 1997; Arco and Aparicio, 2001). However, the load-carrying capacity of the bridge would be greatly reduced because of the eccentric mass. Another effective method is storm rope, which is the connection cable between the pylon foundation (or joint area of cross beam and pylon) and the main cable (or catwalks). Storm rope could increase the natural vertical bending and torsional stiffness, but extra cost and construction time are required.

Storm ropes effectiveness on aerodynamic stability of Xihoumen Bridge is investigated in previous study (Yang et al., 2018). Two anchoring positions were considered. As Fig. 16 shows, cable 1 is anchored at the joint area where the cross beam of pylon exists, while cable 2 is at the base of the pylon. The other end is attached to the main cable and horizontal projection lengths for the two cables are 1/8 of mid-span and 1/4 of mid-span respectively. Table 2 lists all cases that had been analyzed considering anchoring positions and ropes size (1% and 10% of the main cable cross-section area A_c)

The flutter speed improvement with four conditions had been examined in a full aerodynamic model test. Following the symmetric erection sequence, the aerodynamic stability limits of various storm ropes and the original program are presented in Fig. 17. An average increase of 15% flutter speed is achieved. Especially, aerodynamic stability performance from stage 6 to stage 10 has been improved by about 25%.

The effect of the improvement of installing storm rope on reducing flutter probability is analyzed by erection flutter risk box-plot. Flutter speed development during erection and the continuous time-varying extreme wind is coupled in analysis. As Fig. 18 shows, storm ropes reduce 50% average flutter probability during the whole erection process. However, an economical and safe choice hide in this box-plot. Just by modifying the construction timeline, the equivalent counter-flutter safety on reducing flutter performance could be achieved by adding the storm rope. Therefore, if the erection start time is not limited, choosing the optimal timeline is the most economical method to

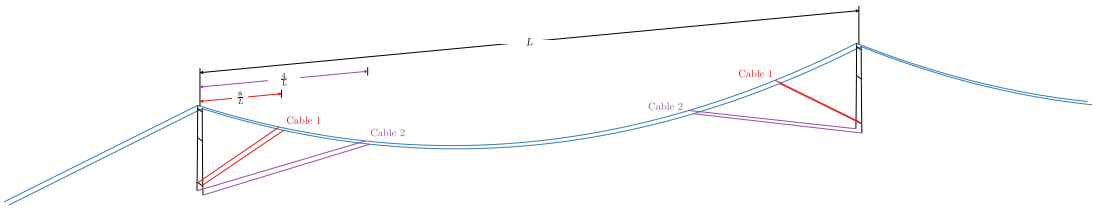

Fig. 16. Configuration of storm ropes during Xihoumen bridge deck erection.

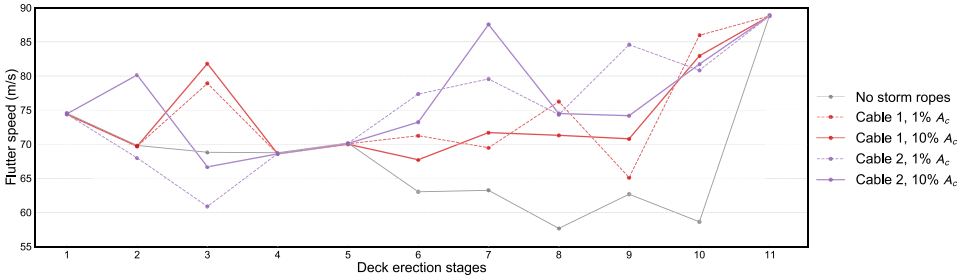

Fig. 17. The evolution of Xihoumen bridge flutter speeds with single storm rope during deck erection.

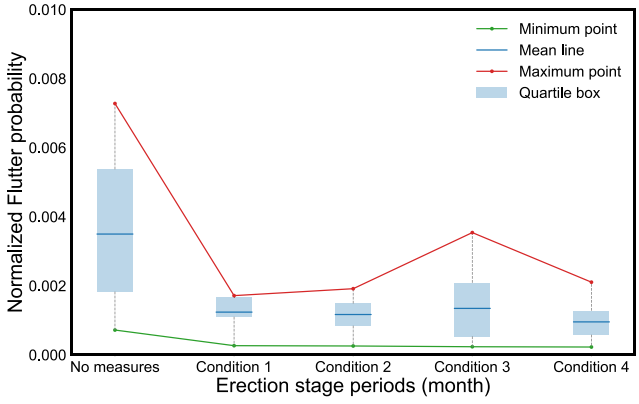

Fig. 18. Normalized flutter risk during erection with different aerodynamic approach (symmetric deck erection program).

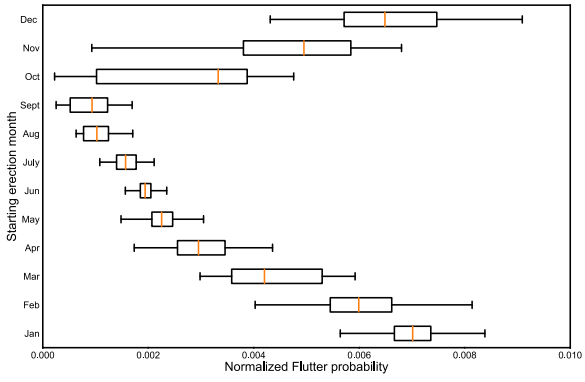

Fig. 19. Normalized flutter risk during erection with different construction site.

improve construction flutter performance than structural approaches. When construction timelines are objectively limited, the adverse start times should also be avoided to maximize the effectiveness of the structural approach.

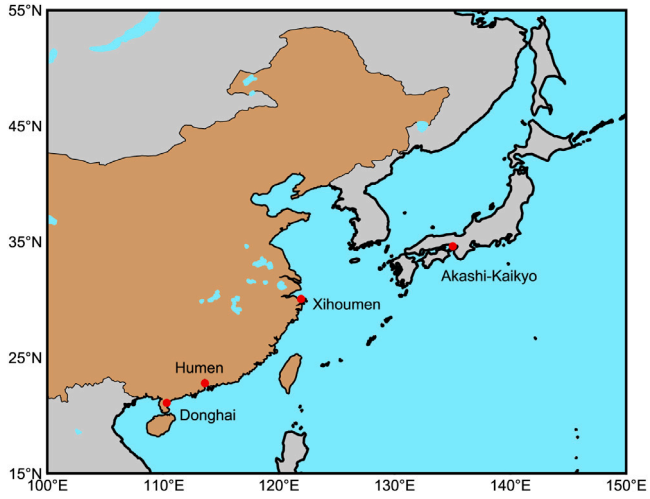

Fig. 20. Coastal long-span suspension bridge construction site map.

5.3. Uncertain erection duration

For a real bridge deck erection program, the schedule should be decided before starting construction. The flutter risk analysis could be done and the best deck erection program could be selected based on the plan. However, there is always a gap between plan and reality, called erection duration uncertain. For example, the erection speed is 1 stage per 30 days in plan, but 1 stage per 27–33 days in reality. In this part, how the erection duration uncertain take influence on the strategy of the deck erection program selection are discussed.

This work assumes that the uncertain erection duration is represented by percentage error which obeys Gaussian distributions with zero mean $N(0, \sigma^2)$. Monte Carlo simulation was used to quantify the influence of construction period disturbance on the total flutter risk. An error coefficient of Gaussian distribution is used to determine the duration of each stage when calculating flutter risk. Here symmetric deck erection program with one stage per month speeding and about 10% percentage error is taken as an example. 10,000 times simulation results of each program are collected, which is shown in Fig. 19. Fig. 19 shows how the uncertainty of the total flutter failure risk is spread out based on a five-number summary (minimum, first quartile (Q1),

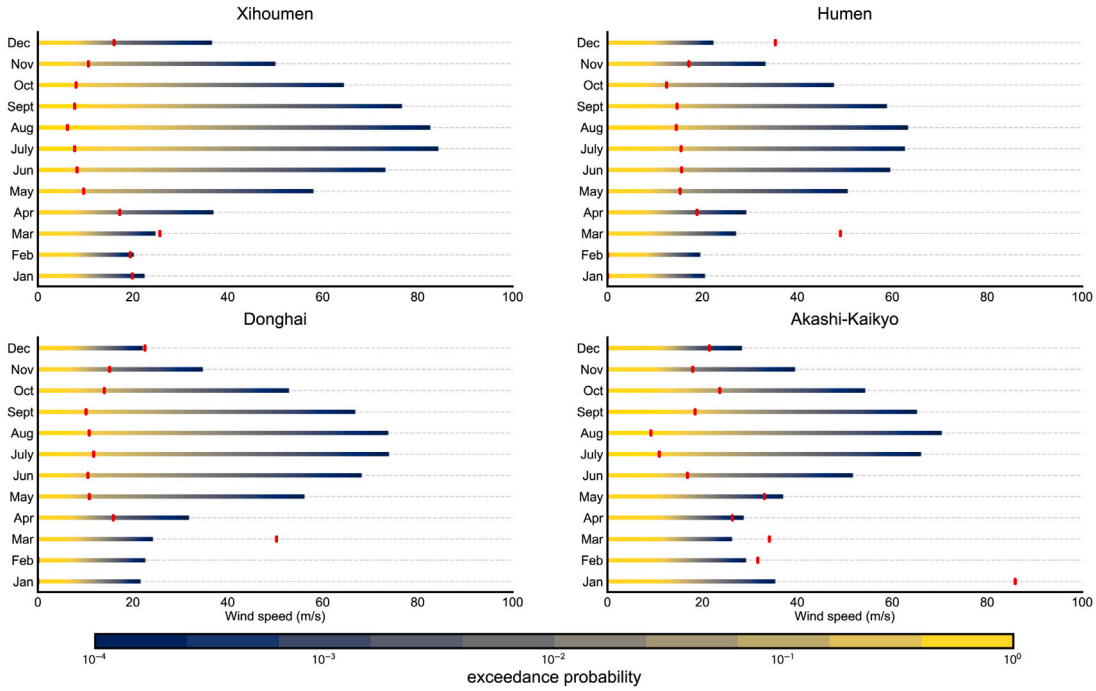

Fig. 21. Mixed wind speed exceeding probability in different months at various construction site (red solid line is the cut-off point of tropical cyclone control and synoptic wind control).

median, third quartile (Q3), and maximum). It could be seen that only 10% deck erection duration error will add 30%–50% fluctuation to flutter risk. In addition, duration uncertain changes the strategy of the deck erection program selection. Q3 or maximum value of Monte Carlo simulation results might be a better metric than the mean value because of the safety. In this case, the optimal deck erection starting month is also August.

5.4. Different construction site

The continuously time-varying suspension bridge critical flutter wind speed and wind environment is the most decisive factor to determine erection timeline on flutter risk. Different wind environments may have different bridge erection strategies. This section discusses how construction sites affect flutter risk by assuming Xihoumen Bridge is built at other coastal suspension bridge sites.

Fig. 20 shows four typical mixed wind climate suspension bridge construction sites, including Xihoumen Bridge, Humen Bridge, Donghai Bridge, and Akashi-Kaikyo Bridge. The mixed wind speed exceeding probability is calculated by mixed wind climate theory as shown in Section 3. Synoptic wind speed data is from NOAA Global Integrated Surface Dataset while tropical cyclone data is from Vickery's full-track simulation model. The extreme-value analysis result is shown in Fig. 21. Four construction sites all have mixed wind environments due to tropical cyclones, but also have some differences between them.

Xihoumen bridge is taken as the typical long-span suspension bridge to find out how different locations affect flutter risk on the erection suspension bridge. Normalized flutter risk during erection with different timelines and programs is calculated and results are shown in Fig. 22. Obviously, the worst wind environment is the construction site of Xihoumen Bridge, while the most favorable place is the Humen Bridge site. Fig. 22 shows the erection bridge of Xihoumen has a similar performance at different places. The optimal asymmetric program is better than symmetric while the mean performance of asymmetric is worse than symmetric. This proves that the evaluation method can be used in different places, and it is a wide applicable method for selecting suspension bridge deck erection strategies.

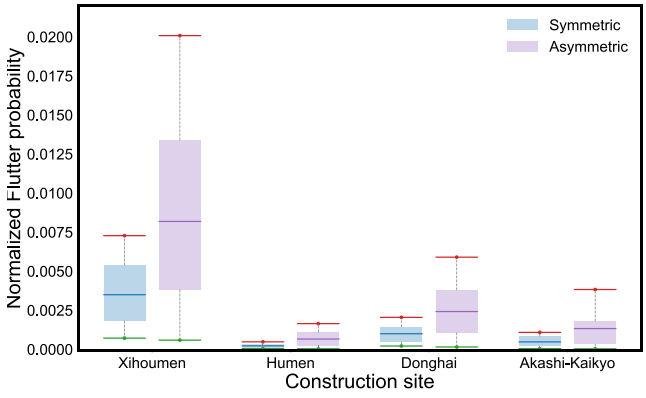

Fig. 22. Normalized flutter risk during erection with different construction site.

6. Conclusion

This paper presents a long-span suspension bridge deck erection plan selection and optimization strategy considering the minimum flutter risk during the whole erection stages. The process of time-dependent flutter failure probability is calculated by considering the mixed climate wind environment including tropical cyclones and monsoon and the continuous time-varying bridge structural states. Two specific analysis methods and visualizations are proposed in this research. Flutter risk flow is used to describe single program flutter performance and erection flutter risk box-plot is a horizontal comparison tool of different erection processes.

Xihoumen Bridge at Chinese coastal is a calculation example in this research. Flutter speeds of different stages are tested by aerodynamic full-model wind tunnel test. The mixed wind speed exceeding probability is calculated by mixed wind climate theory. Synoptic wind speed data is from NOAA Global Integrated Surface Datasets while tropical cyclone data is from Vickery's full-track simulation model. The optimal

timeline for Xihoumen Bridge is starting in August and one-month duration for each stage.

Deck erection timeline plays a key role in flutter risk. 40 times difference on flutter risk exists between the best and worst timeline. If construction timeline is not limited, this research proves that timeline optimization is a more economical and safe approach than structural approaches like storm ropes. When construction timelines are objectively limited, the adverse start times should also be avoided to maximize the effectiveness of the structural approach.

Deck erection plan horizontal comparison could not only focus on the lowest flutter speed but the flutter risk probability for all timelines. Erection risk box-plot is an effective tool in this case. If the erection starting time is free, the minimum flutter probability should be the indicator. The mean-value and quartile box should be paid more attention to when a timeline is unknown.

CRediT authorship contribution statement

Ma Teng: Methodology, Writing – original draft, Formal analysis, Software, Visualization. **Cui Wei:** Project administration, Conceptualization, Writing – review & editing. **Zhao Lin:** Writing – review & editing, Funding acquisition. **Yang Yongxin:** Resources, Investigation. **Ge Yaojun:** Supervision.

Declaration of competing interest

The authors declare that they have no known competing financial interests or personal relationships that could have appeared to influence the work reported in this paper.

Acknowledgments

The authors gratefully acknowledge the support of National Natural Science Foundation of China (52078383, 52008314, 51978527) and Independent subject of State Key Lab of Disaster Reduction in Civil Engineering (SLDRCE19-B-11). Any opinions, findings and conclusions are those of the authors and do not necessarily reflect the reviews of the above agencies.

References

Amman, O.H., von Kármán, T., Woodruff, G.B., 1941. The failure of the Tacoma Narrows bridge.

Tanaka, H., Larose, G., Kimura, K., 1998. Aerodynamics of long-span bridges during erection. Bridge Aerodyn. 119–127.

Smith, I., 1964. The Aeroelastic Stability of the Severn Suspension Bridge. National Physical Laboratory, Aerodynamics Division, Department of.

Larsen, A., 1993. Aerodynamic aspects of the final design of the 1624 m suspension bridge across the Great Belt. J. Wind Eng. Ind. Aerodyn. 48 (2–3), 261–285.

Yang, Y., Zhang, L., Ding, Q., Ge, Y., 2018. Flutter performance and improvement for a suspension bridge with central-slotted box girder during erection. J. Wind Eng. Ind. Aerodyn. 179, 118–124.

Ge, Y., Tanaka, H., 2000. Aerodynamic stability of long-span suspension bridges under erection. J. Struct. Eng. 126 (12), 1404–1412.

Svensson, H.S., Kovacs, I., 2017. Examples of analytical aerodynamic investigations of long-span bridges. In: Aerodynamics of Large Bridges. Routledge, pp. 171–182.

Larsen, A., 1997. Prediction of aeroelastic stability of suspension bridges during erection. J. Wind Eng. Ind. Aerodyn. 72, 265–274.

Arco, D.C.d., Aparicio, A.C., 2001. Improving the wind stability of suspension bridges during construction. J. Struct. Eng. 127 (8), 869–875.

Chen, A., Xiang, H., Song, J., 1997. Wind resistant researches on Tigergate suspension bridge in typhoon-prone area. In: Proc., 2nd Eur. African Conf. on Wind Engrg. Servisi Grafici Editoriale, Padova, Italy, pp. 1433–1440.

Miyata, T., Yamaguchi, K., 1993. Aerodynamics of wind effects on the Akashi Kaikyo Bridge. J. Wind Eng. Ind. Aerodyn. 48 (2–3), 287–315.

Bakis, K., Limebeer, D., Williams, M., Graham, J., 2016. Passive aeroelastic control of a suspension bridge during erection. J. Fluids Struct. 66, 543–570.

Habte, F., Chowdhury, A.G., Yeo, D., Simiu, E., 2015. Wind directionality factors for nonhurricane and hurricane-prone regions. J. Struct. Eng. 141 (8), 04014208.

Cui, W., Ma, T., Zhao, L., Ge, Y., 2021. Data-based windstorm type identification algorithm and extreme wind speed prediction. J. Struct. Eng. 147 (5), 04021053.

Chen, G., Lombardo, F.T., 2020. An automated classification method of thunderstorm and non-thunderstorm wind data based on a convolutional neural network. J. Wind Eng. Ind. Aerodyn. 207, 104407.

Gomes, L., Vickery, B., 1978. Extreme wind speeds in mixed wind climates. J. Wind Eng. Ind. Aerodyn. 2 (4), 331–344.

Young, A.H., Knapp, K.R., Inamdar, A., Hankins, W., Rossow, W.B., 2018. The international satellite cloud climatology project H-Series climate data record product. Earth Syst. Sci. Data 10 (1), 583–593.

Vickery, P.J., Skerlj, P., Steckley, A., Twisdale, L., 2000b. Hurricane wind field model for use in hurricane simulations. J. Struct. Eng. 126 (10), 1203–1221.

Vickery, P., Skerlj, P., Twisdale, L., 2000a. Simulation of hurricane risk in the US using empirical track model. J. Struct. Eng. 126 (10), 1222–1237.

Scanlan, R.H., Simiu, E., 1996. Wind Effects on Structures: Fundamentals and Applications to Design. Wiley, New York.

Georgiou, P.N., 1986. Design wind speeds in tropical cyclone-prone regions.

Cui, W., Caracoglia, L., 2019. A new stochastic formulation for synthetic hurricane simulation over the North Atlantic Ocean. Eng. Struct. 199, 109597.

Fang, G., Pang, W., Zhao, L., Rawal, P., Cao, S., Ge, Y., 2021. Toward a refined estimation of typhoon wind hazards: Parametric modeling and upstream terrain effects. J. Wind Eng. Ind. Aerodyn. 209, 104460.

Chu, X., Cui, W., Zhao, L., Cao, S., Ge, Y., 2021. Probabilistic flutter analysis of a long-span bridge in typhoon-prone regions considering climate change and structural deterioration. J. Wind Eng. Ind. Aerodyn. 215, 104701.

Gimsing, N.J., Georgakis, C.T., 2011. Cable Supported Bridges: Concept and Design. John Wiley & Sons.

Tanaka, H., Gimsing, N., 1999. Aerodynamic stability of non-symmetrically erected suspension bridge girders. J. Wind Eng. Ind. Aerodyn. 80 (1–2), 85–104.

Cook, N., 1982. Towards better estimation of extreme winds. J. Wind Eng. Ind. Aerodyn. 9 (3), 295–323.

Harris, R., 1999. Improvements to themethod of independent storms'. J. Wind Eng. Ind. Aerodyn. 80 (1–2), 1–30.

Gumbel, E.J., 2004. Statistics of Extremes. Courier Corporation.

ASCE, ASCE, 2016. Minimum Design Loads for Building and Other Structures (ASCE 7-16). American Society of Civil Engineers.

Ministry of Transports of the People's Republic of China, Ministry of Transports of the People's Republic of China, 2018. Wind-Resistant Design Specification for Highway Bridges (JTG/T 3360-01-2018). Ministry of Transports of the People's Republic of China.

Brancaleoni, F., Brotton, D., 1981. Analysis and prevention of suspension bridge flutter in construction. Earthq. Eng. Struct. Dyn. 9 (5), 489–500.